Effective Width in Shear of Reinforced Concrete Solid Slab Bridges under Wheel Loads

By

Eva O.L. Lantsoght, Postdoctoral Researcher, Delft University of Technology, Department of Design & Construction – Concrete Structures, St II 2.06, Stevinweg 1, 2628 CN Delft, The Netherlands, 0031 15 2787449, E.O.L.Lantsoght@tudelft.nl (corresponding author),

Ane de Boer, Senior Adviser, Ministry of Infrastructure and the Environment, Department of Infrastructure, H9, P.O. Box 24057, 2502MB Utrecht, The Netherlands, ane.de.boer@rws.nl,

Cor van der Veen, Associate Professor, Delft University of Technology, Department of Design & Construction – Concrete Structures, St II 2.05, Stevinweg 1, 2628 CN Delft, The Netherlands, 0031 15 2784577, C.vanderveen@tudelft.nl, and

Joost C. Walraven, Emeritus Professor, Delft University of Technology, Department of Design & Construction – Concrete Structures, St II 2.04, Stevinweg 1, 2628 CN Delft, The Netherlands, 0031 15 2785452, J.C.Walraven@tudelft.nl

Submission Date: 28/10/2013

Word Count: 4991 words (text) + 2500 word equivalents (3 tables and 7 figures 250 wc each) = 7491 words

Effective Width in Shear of Reinforced Concrete Solid Slab Bridges under Wheel Loads

1
2
3 **ABSTRACT**
4
5 For the assessment of reinforced concrete slab bridges in the Netherlands, the shear stress
6 resulting from the dead loads and live loads is determined in a spreadsheet or from a finite
7 element model. In a spreadsheet-based approach, an assumption for the distribution of the loads
8 from the wheel prints is necessary. When finite element methods are used, it is necessary to
9 determine over which length (a multiple of the effective depth) the peak shear stress can be
10 distributed for comparison to the design shear capacity.
11   To recommend a load-spreading method, experiments were executed on slab strips of
12 increasing widths. The shear capacity did not increase with the increasing width upon passing a
13 threshold. This threshold is compared to different load spreading methods, indicating that a
14 distribution from the far side of the wheel print is to be preferred. This recommendation is also
15 supported by the results of a statistical analysis and the stress distribution in nonlinear finite
16 element models.
17   To find the distribution width in a finite element method, a numerical model is compared
18 to an experiment on a slab subjected to a concentrated load in which the support consists of a line
19 of 7 bearings equipped with load cells measuring the reaction forces. These measurements were
20 compared to the stress profile at the support from the model, showing that the peak can be
21 distributed over 4 times the effective depth.
22   These recommendations for the effective width and distribution width are research-based
23 tools that replace the previously used rules of thumb resulting from engineering judgement.
24

1 **INTRODUCTION**
2 As a result of the increased live loads prescribed by the recently implemented EN 1991-2:2003
3 (*1*) and the smaller allowable shear capacities from EN 1992-1-1:2005 (*2*), a large number of
4 existing solid slab bridges in the Netherlands is subject to discussion. In total, about 600 slab
5 bridges are assumed to be shear-critical. The majority of these bridges have 3 to 4 spans and a
6 constant slab depth. The average main span is 13.5 m (44.3 ft), the average end span is 10.1 m
7 (33.1 ft) and the average total slab width equals 13.2 m (43.3 ft). About 60% of these bridges
8 were built before 1976.
9   In a first round of assessments, the solid slab bridges were checked in a spreadsheet-
10 based method, the "Quick Scan". This approach was originally developed in the mid-2000s by
11 engineering offices in the Netherlands, and is similar to a hand calculation. The result of the
12 Quick Scan is a "Unity Check": the ratio between the shear stress at the edge of the support due
13 to the composite dead load (self-weight and wearing surface) and the live loads (from Load
14 Model 1, EN 1991-2:2003 (*1*)) and the shear capacity as prescribed by EN 1992-1-1:2005 (*2*).
15 For concentrated loads, it is necessary to determine the effective width associated with the axle
16 loads from the live load model.
17   When the Unity Check value from the Quick Scan is larger than 1, a more refined
18 analysis is necessary. A finite element calculation is then used. In the model, the composite dead
19 load and live loads from Load Model 1 are applied, and the load combination that results in the
20 largest shear stress at the support is sought. This shear stress then needs to be compared to the
21 shear capacity from EN 1992-1-1:2005 (*2*).
22   When using the Quick Scan approach, the most unfavorable position of the design trucks
23 needs to be assumed, and, for the case of a symmetric, 3-span structure, the method can be
24 limited to at least 3 sections at which the Unity Check is carried out. These limitations are
25 omitted when using a finite element model. In the Quick Scan sheet, a number of conservative
26 assumptions, covering the range of slab bridges under study, are used. With a finite element
27 verification, a more tailored approach is possible. As prescribed by the different levels of
28 approximation from the *fib* Model Code 2010 (*3*), a level II method, such as an assessment based
29 on a finite element model, will be more cost- and time-consuming as compared to a level I
30 method, such as the Quick Scan sheet, but will lead to a result that is closer to the real capacity of
31 the element or structure under study.
32   The objective of this paper is to study the distribution at the support of the shear stresses
33 originating from the concentrated loads. For the Quick Scan approach an effective width over
34 which the concentrated loads can be distributed at the support is necessary. For the finite element
35 models, it is necessary to quantify the width over which the peak shear stress can be distributed
36 for comparison to the shear capacity predicted by the code.
37
38 **CURRENT PRACTICE AND OUTLOOK**
39 **Effective Width in Shear**
40 In slabs and wide beams subjected to a concentrated load, the width at the support that carries the
41 shear loading needs to be estimated; this width is the effective width in shear b_{eff}. Theoretically,
42 the effective width b_{eff} is determined so that the total shear stress over the support equals the
43 maximum shear stress over the effective width (*4*). For calculations, the determination of this
44 width depends on local practice: either a fixed width (for example, 1 m = 3.3 ft) is used or a
45 horizontal load spreading method is used. Different load spreading methods are used in practice:
46 from the center of the load to the face of the support under an angle of 45$^\text{o}$ as used in Dutch

1   practice, resulting in the effective width b_{eff1} (Fig. 1a), from the far side of the load to the face of
2   the support under 45° as used in French practice (5) (Fig. 1b) or with an angle depending on the
3   type of support and to a certain distance away from the support as prescribed by the Model Code
4   2010 (3) (Fig. 1c). To improve the Quick Scan method, it is necessary to study the effective
5   width for slabs in one-way shear subjected to a concentrated load based on experiments.
6
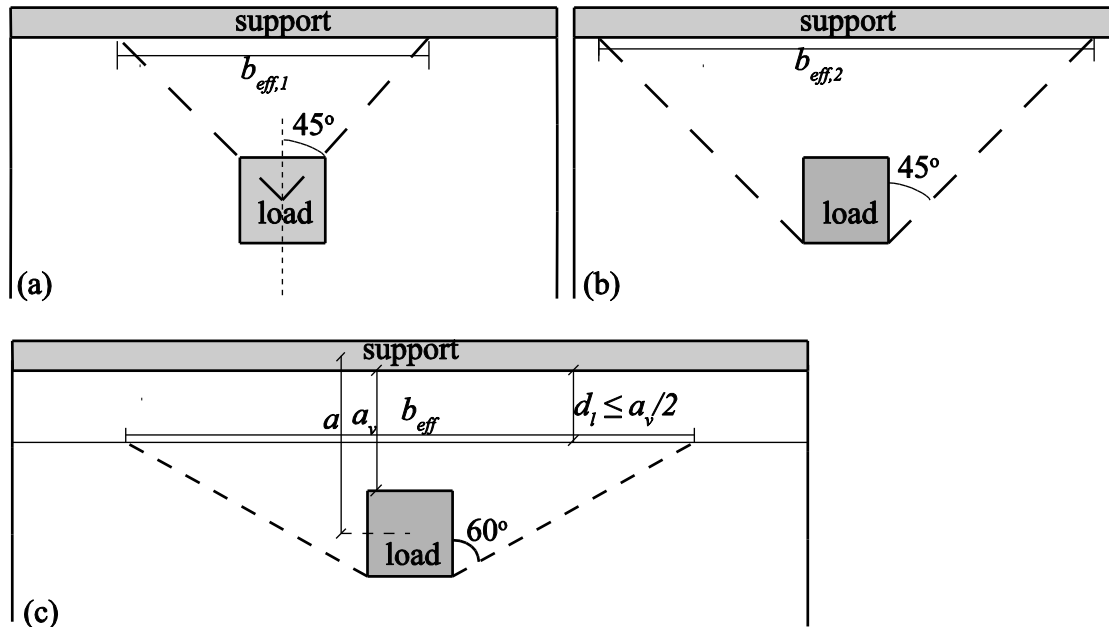
7   (c)
8   **FIGURE 1 Top view of slab showing determination of effective width (a) assuming 45°**
9   **horizontal load spreading from the center of the load: b_{eff1}; (b) assuming 45° horizontal**
10   **load spreading from the far corners of the load: b_{eff2}; (c) load spreading as recommended**
11   **by *fib* Model Code 2010 for loads near to simple supports.**
12

13   **Distribution Width for Finite Element Calculations**
14   When a finite element calculation is used, the shear stress at the support will not be constant over
15   the entire width of the support, but, due to the presence of the wheel loads, will have a peak
16   value. Typically in an assessment, this peak shear stress is distributed over a certain width. The
17   value of this width depends on local practice, and can be a fixed value, such as 1 m (3.3 ft), or a
18   multiple of the effective depth to the longitudinal reinforcement d_l. In Dutch practice, the peak
19   shear stress is distributed over $2d_l$. The average stress value over the distribution width is then
20   used for comparison to the prescribed shear capacity. To gain a better insight in the distribution
21   width, measurements of the reaction force distribution from experiments are necessary.
22

23   **EXPERIMENTS**
24   To determine an approximate method for the effective width in shear, a series of experiments on
25   slabs and slab strips subjected to a concentrated load is carried out. To study the distribution of
26   the peak shear stress over the support, an experiment is carried out on a slab subjected to a
27   concentrated load in which the support line consists of bearings equipped with load cells
28   measuring the reaction forces.
29   The slabs that are tested represent a half-scale model of a continuous reinforced concrete
30   slab bridge. The experimental work comprises 26 slabs (S-series) of 5 m × 0.3 m × 2.5 m (16 ft ×

1   1 ft × 8 ft) and 12 slab strips (B-series) of 5 m × 0.3 m (16 ft × 1 ft) with a variable width ranging
2   from 0.5 m (1.6 ft) to 2 m (6.6 ft) in increments of 0.5 m (1.6 ft). For the effective width, the
3   results from the slab strips are analyzed as well as the results from the first 18 slabs. For the
4   study of the distribution width over the support, S25, a slab subjected to a concentrated load only
5   and supported by a line of bearings equipped with load cells, is studied in particular. In Fig. 2a, a
6   top view of the test setup is shown. A load close to the support is applied, as this case results in
7   the largest shear stresses for assessment.
8
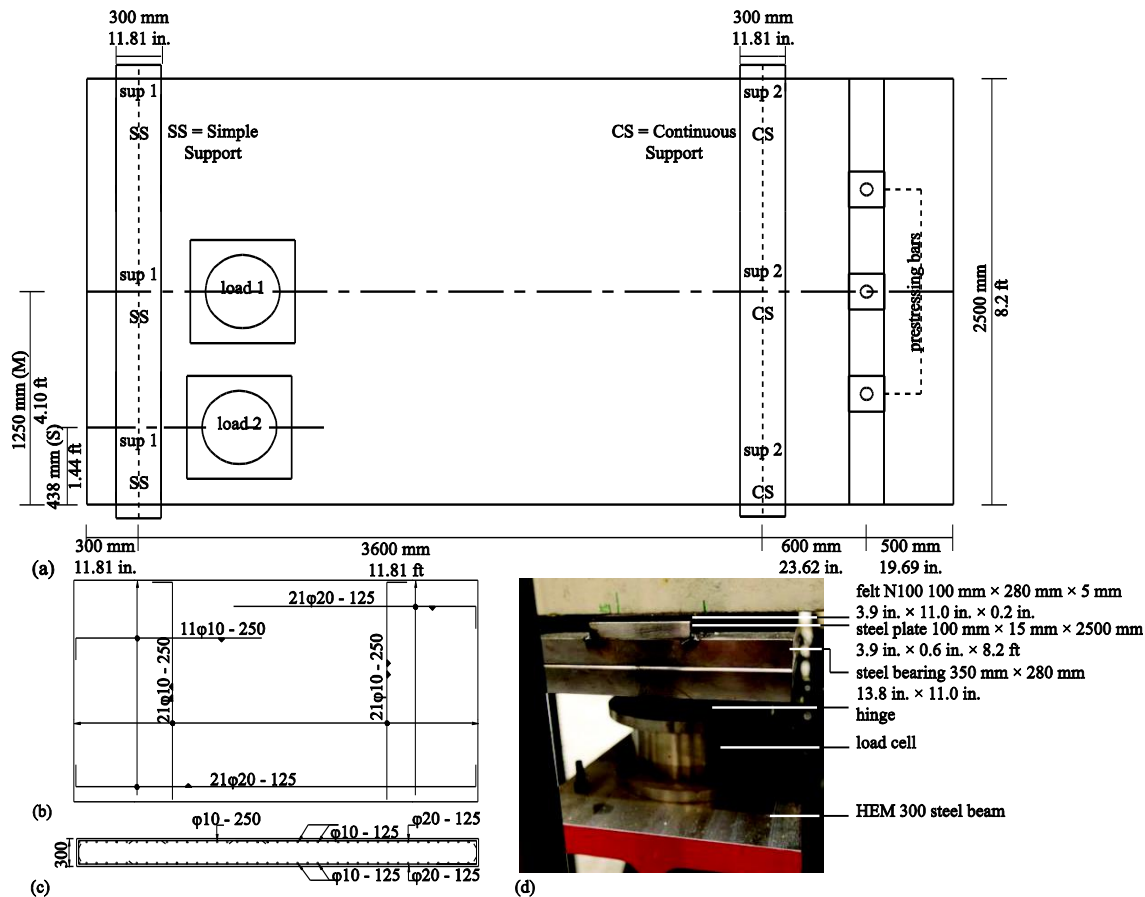
10   **FIGURE 2   Experimental setup and specimens: (a) top view of setup, (b) top view of**
11   **reinforcement layout and (c) cross-section of reinforcement layout for S3, S5-S10, S19-S26**
12   **(in [mm]: 1 mm = 0.04 in.); (d) detail of support bearing as used in S25T1 to measure**
13   **distribution of reaction forces over support.**
14
15   To study the distribution of the peak shear stress over the support, experiment S25T1 is analysed.
16   In this experiment, each support line consisted of 7 steel bearings (Fig. 2d) equipped with load
17   cells and hinges. The 300 mm × 300 mm (11.8 in. × 11.8 in.) concentrated load was placed in the
18   middle of the width near to the simple support (SS), sup 1 in Fig. 2a. The reinforcement of S25 is
19   as shown in Fig. 2b and Fig. 2c, resulting in a longitudinal reinforcement ratio ρ_l = 0.996% and a
20   transverse flexural reinforcement ratio ρ_t = 0.258%. Normal strength concrete of class C28/35
21   with glacial river aggregates of maximum 16 mm (0.63 in.) was used. The cube concrete
22   compressive strength at the age of testing (170 days) was $f_{c,cube}$ = 58.57 MPa (8.5 ksi) and the

1 tensile splitting strength was f_{ct} = 4.47 MPa (648 psi). In S25T1, failure occurred for a maximum
2 concentrated load of P_u = 1461 kN (328 kip). This load results in a shear stress of 2.53 MPa (367
3 psi) when b_{eff1} is used or 1.64 MPa (238 ksi) when b_{eff2} is used. The shear capacity predicted
4 according to EN 1992-1-1:2005 was 1.02 MPa (148 psi). After the experiment, mostly
5 longitudinal cracks were observed on the bottom of the slab, as well as some punching damage.
6 On the side faces no cracks were visible, not even flexural cracks. Further discussion of the
7 individual tests of S1 to S10 and the slab strips (*6*), S11 to S14 (*7*), S15 to S18 (*8*) and S19 to
8 S26 (*9*) are reported elsewhere.
9
10 **FINITE ELEMENT MODEL**
11 The experiment is simulated in DIANA, Release 9.4.4 (*10*) by using a linear finite element
12 model. The slab was modeled as shell elements and the supports were modeled as 3D solid
13 elements (Fig. 3). In between the solid and shell elements, interface elements representing the
14 layer of felt were used. For the model of the slab, 40% of orthotropy was assumed. The load was
15 modeled as 300 mm × 300 mm (11.8 in. × 11.8 in.), as in the experiment. During the experiment,
16 the slab did not touch all support bearings due to initial geometric imperfections.
17 Therefore, based on the measurements of the reaction forces in the supports, a phased activation
18 of the supports was also simulated in the model.
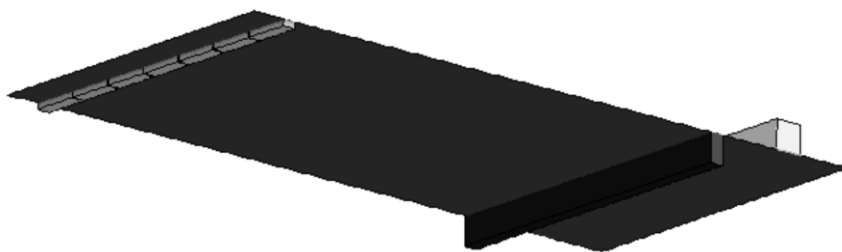
19
20 **FIGURE 3 Overview of the finite element model**
21
22 **RECOMMENDATIONS**
23 **Effective Width in Quick Scan**
24 *Based on the Experiments of Specimens with a Different Width*
25 In the series of experiments on specimens with a varying width, slabs and slab strips with a width
26 between 0.5 m (1.6 ft) and 2.5 m (8.2 ft) were studied. Six different loading conditions were
27 applied to the specimens for each studied width. According to the concept of the effective width
28 in shear based on a load spreading method (Fig. 1), it should be possible to distinguish a
29 threshold effective width in a series of specimens with an increasing width. For the specimens
30 with a small width, an increase in the width corresponds to an increase in the shear capacity, as
31 the full width of the specimen is activated to carry the shear. After reaching a threshold, larger
32 widths will no longer result in larger shear capacities, as only the effective width at the support is
33 activated to carry the shear.
34   The resulting shear capacity V_{exp} of the experiments on the slab strips with an increasing
35 width b is shown in Fig. 4. For every width, 6 sets of geometric properties are tested, as shown
36 by the legend of Fig. 4 and the "Series" column of Table 1. six different loading situations are
37 studied for each specimen width that is tested. The concentrated load was placed at two different
38 locations close to the support: at a distance a (center-to-center distance between the load and the
39 support) of 400 mm (15.7 in.; resulting in a/d_l = 1.51) or 600 mm (23.6 in.; resulting in a/d_l =

1   2.26). Two sizes of the concentrated load are tested: 200 mm × 200 mm (7.9 in. × 7.9 in., half-
2   scale wheel load from Load Model 1 from EN 1991-2:2003) and 300 mm × 300 mm (11.8 in. ×
3   11.8 in.). As shown in Fig. 2a, the influence of the moment at the support is studied by testing at
4   the simple support (SS) and at the continuous support (CS). The lines in Fig. 4 show the trend of
5   the data: the inclined lines show the trendline through the datapoints for which the shear capacity
6   is still increasing and the horizontal lines show the average shear capacity when no further
7   increase is observed. The intersection of the inclined trendline and the horizontal line gives the
8   threshold effective width of a series of specimens with increasing width. The experiments indeed
9   confirm the existence of a threshold width, which can be compared to the results for the effective
10 width based on the load spreading methods from Fig. 1. The results of this comparison are given
11 in Table 1, in which:
12 b_{meas} threshold effective width from the experiments;
13 b_{eff1} effective width based on the Dutch load spreading method;
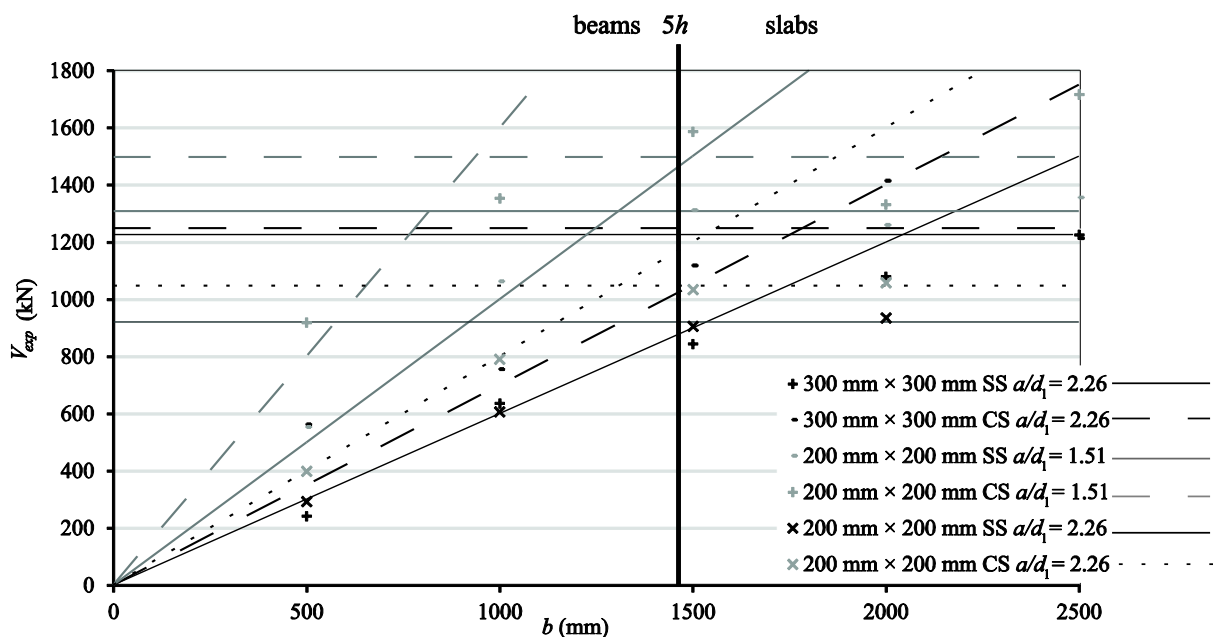14 b_{eff2} effective width based on the French load spreading method.
15

16
17 **FIGURE 4 Results for maximum sectional shear V_{exp} at the support in experiments on slab**
18 **strips and slabs with a width b between 0.5 m (1.6 ft) and 2.5 m (8.2 ft), also showing the**
19 **distinction between beams and slabs at $5h$ from EN 1992-1-1:2005 (2), with h = the**
20 **specimen height.**
21 **NOTE: 1 mm = 0.04 in., 1 kN = 0.225 kip.**
22
23 It can be seen in Table 1 that the threshold effective width most closely resembles the effective
24 width based on the French load spreading method b_{eff2}. Based on the experiments, it can be
25 recommended to use the French load spreading method. This method correctly takes into account
26 the influence of the size of the load, as well as the distance between the load and the support. It
27 does not take into account the smaller effective threshold width that is observed at the continuous
28 support as compared to the simple support, resulting in lower values for b_{meas}/b_{eff2} at the
29 continuous support.
30

1
2 **TABLE 1 Effective width as calculated from the experimental results.**

No	Series	b_{meas} (m)	b_{eff1} (m)	b_{eff2} (m)	b_{meas}/b_{eff1} Dutch	b_{meas}/b_{eff2} French
1	300 mm × 300 mm, SS, $a/d_l = 2.26$	2.04	1.1	1.7	1.86	1.20
2	300 mm × 300 mm, CS, $a/d_l = 2.26$	1.78	1.1	1.7	1.62	1.05
3	200 mm × 200 mm, SS, $a/d_l = 1.51$	1.31	0.7	1.1	1.87	1.19
4	200 mm × 200 mm, CS, $a/d_l = 1.51$	0.94	0.7	1.1	1.34	0.85
5	200 mm × 200 mm, SS, $a/d_l = 2.26$	1.53	1.1	1.5	1.39	1.02
6	200 mm × 200 mm, CS, $a/d_l = 2.26$	1.31	1.1	1.5	1.19	0.87

3 **NOTE: 1 m = 3.3 ft., 1 mm = 0.04 in.**
4
5 *Based on a Statistical Analysis of the Ratio between the Experimental and Predicted Capacities*
6 In a next step, a statistical analysis of the ratio between the experimental results and the predicted
7 values from EN 1992-1-1:2005 (*2*) with b_{eff1} and b_{eff2}, is used. To determine the predicted shear
8 capacity, the constant $C_{Rd,c}$ is taken as 0.15 (*11*), mean material properties are used and all partial
9 factors equal 1. For loads applied within a face-to-face distance a_v between the load and the
10 support of $0.5d_l \leq a_v \leq 2d_l$ from the edge of the support, the contribution to the resulting shear
11 force is multiplied by $\beta = a_v/2d_l$, as prescribed by §6.2.2.(6) from EN 1992-1-1:2005 (*2*). All
12 experiments on slabs and slab strips under concentrated loads are analyzed as well as a subset of
13 27 experiments on slabs that failed in wide beam shear. This subset is gathered from a database
14 of 215 experiments on slabs as reported in the literature (*12*). The results of the statistical
15 analysis of the ratio between the experimental results to the predicted values are given in Table
16 2, with:
17 V_{TU} the ultimate shear force as observed in the Delft University of Technology
18   experiments;
19 V_{db} the ultimate shear force from the 27 experiments selected from the slab database;
20 $V_{EC,beff1}$ the shear capacity as calculated from EN 1992-1-1:2005 (*2*) using the Dutch load
21   spreading method resulting in b_{eff1}, and
22 $V_{EC,beff2}$ the shear capacity as calculated from EN 1992-1-1:2005 (*2*) using the French load
23   spreading method resulting in b_{eff2};
24 AVG   average value of the studied ratio;
25 STD   standard deviation of the studied ratio;
26 COV   coefficient of variation of the studied ratio;
27 Char   characteristic value (5% lower bound assuming a normal distribution) of the
28   studied ratio.
29 The analysis in Table 2 indicates that the French load spreading method is to be preferred as it
30 leads to a smaller underestimation of the capacity and a smaller coefficient of variation for the
31 Delft experiments; and a smaller coefficient of variation for the experiments from the slab shear
32 database. The results based on the experiments from the slab shear database however indicate
33 that unsafe predictions can result, as not all parameters that influence the shear capacity are taken
34 into account in the expression for the shear capacity from EN 1992-1-1:2005 (*2*) in an adequate
35 manner. The difference in the results between two sets of data can be explained by
36 acknowledging that the experiments at TU Delft were carried out with the concentrated load
37 close to the support, for which the beneficial effect of direct load transfer increased the shear
38 capacity as compared to the experiments from the database.

1
2 **TABLE 2 Comparison between EN 1992-1-1:2005 (*2*) and the experimental results from**
3 **the experiments carried out at Delft University of Technology and as reported in the**
4 **literature**

	Delft Experiments		Subset from Slab Shear Database	
	$V_{TU}/V_{EC,beff1}$	$V_{TU}/V_{EC,beff2}$	$V_{db}/V_{EC,beff1}$	$V_{db}/V_{EC,beff2}$
AVG	3.40	2.38	2.17	1.38
STD	0.89	0.52	1.02	0.46
COV	26%	22%	47%	33%
Char	1.94	1.53	0.50	0.63

5
6 *Based on Nonlinear Finite Element Calculations*
7 As a final verification of the effective width that is recommended for use in the Quick Scan
8 method, the stress distribution at the support in nonlinear finite element models was studied. In a
9 series of nonlinear finite element models with a variable width and shear span (*13*), the effective
10 width at the support was studied based on the shear stress distribution over the support. This
11 analysis showed that the French load spreading method, resulting in b_{eff2}, gives mostly a safe
12 average of the effective width, although the increase of the effective width for an increasing
13 shear span is smaller in the models than as found when using the French load spreading method.
14 In this series of models, the effective width was also found to be slightly dependent on the
15 overall slab width. Overall, the nonlinear finite element models indicated that, within the scope
16 of the Quick Scan, the effective width b_{eff2} from the French load spreading method leads to better
17 results than the previously used load spreading method.
18
19 *Application to Solid Slab Bridges Verified based on the Quick Scan*
20 The French load spreading method can be applied to the wheel loads from Load Model 1, EN
21 1991-2:2003 (*1*), for both wheel loads of each axle. For loads near to the free edge of a slab, an
22 asymmetric effective width can be used, limited by the edge distance on one side and on the
23 other side by the width determined based on the load spreading method. While this
24 approximation results in an unbalance between the location of the reaction forces of the load and
25 of the shear distribution at the support, it was found that such a distribution statistically leads to
26 better results (*12*). As a result, for the axles in the first lane, an asymmetric effective width can
27 be used.
28   As the French horizontal load spreading method results in overlapping effective widths
29 when considering each wheel load of the axle separately, it is a conservative approach to
30 determine the effective width of the entire axle (two wheel loads combined). As in Load Model 1
31 always two wheel loads per axle are considered, using the effective width associated with the
32 axle is a more conservative approach than using the effective width per concentrated load. There
33 are however no experimental results available to actually study the load-spreading behaviour for
34 a slab subjected to two concentrated loads or four concentrated loads (two axles at 1.2 m = 3.94
35 ft distance of each other).
36
37
38
39
40

1 **Distribution Width at Support in Finite Element Analysis**
2 *Measured Reaction Forces in Experiment and Verification in Finite Element Model*
3 For the application of the second level of approximation based on the resulting shear stress at the
4 support from a finite element analysis, the distribution width should be studied. To determine
5 this width, the question was over which distance αd_l, with α a constant ≥ 2, the peak shear stress
6 should be distributed.
7   At the simple support line of S25T1, 7 load cells (Fig. 5a) were used to continuously
8 measure the reaction force at different positions along the support during the experiment. Nine
9 levels of the applied loading in increments of 10% of the ultimate load (up to 90% of the ultimate
10 load on the slab) are used. The final interval from 90% to 100% of the ultimate load is not
11 considered because the occurring failure cracking cannot be represented correctly by the linear
12 finite element model that is used for the comparison. The measured reaction forces in the load
13 cells are given in Fig. 5a.
14   The reaction forces at the supports in the constructed finite element model are used as an
15 indicator for the quality of the model, and to validate the model. The reaction forces from the
16 model as given in Fig. 5b can be compared to the measured forces from Fig. 5a. In both figures,
17 the same nine intervals of the applied load are considered. The comparison between Fig. 5a and
18 Fig. 5b shows that the performance of the finite element model is satisfactory and that the model
19 can be used to study the distribution width of the peak shear stresses.
20
21 *Shear Stress Analysis*
22 The results of the reaction forces as measured by the load cells are translated into shear stresses
23 for the analysis. Two levels of the load are considered: a maximum load of $F_{jack} = 585$ kN (132
24 kip; 40% of the ultimate load) and $F_{jack} = 1314$ kN (296 kip; 90% of the ultimate load). The
25 method is illustrated for a concentrated load of $F_{jack} = 1314$ kN (296 kip). The reaction forces FSi
26 with i from 0 to 6 are measured at discrete locations (arrows in Fig. 6), the positions of the load
27 cells, along the slab width. To find the total reaction force $F_{tot,2d}$ and $F_{tot,4d}$ over $2d_l$ and $4d_l$
28 respectively, it is assumed that the reaction force is distributed uniformly over the corresponding
29 influence length of the support (Fig. 6a and Fig. 6b). The distance $2d_l$ or $4d_l$ is assumed around
30 the center of the middle load cell (FS3). Based on the measurements, the total applied reaction
31 force, $F_{tot,2d}$ over $2d_l$ is:

32
$$F_{tot,2d} = FS3 + \frac{86 \text{ mm}}{358 \text{ mm}}(FS2 + FS4) = 580 \text{ kN} = 130 \text{ kip} \qquad (1)$$

33 The average shear stress τ_{2d} over $2d_l$ can thus be defined as:

34
$$\tau_{2d} = \frac{F_{tot,2d}}{2d_l^2} = \frac{580 \text{ kN}}{2(265 \text{ mm})^2} = 4.13 \text{ MPa} = 599 \text{ psi} \qquad (2)$$
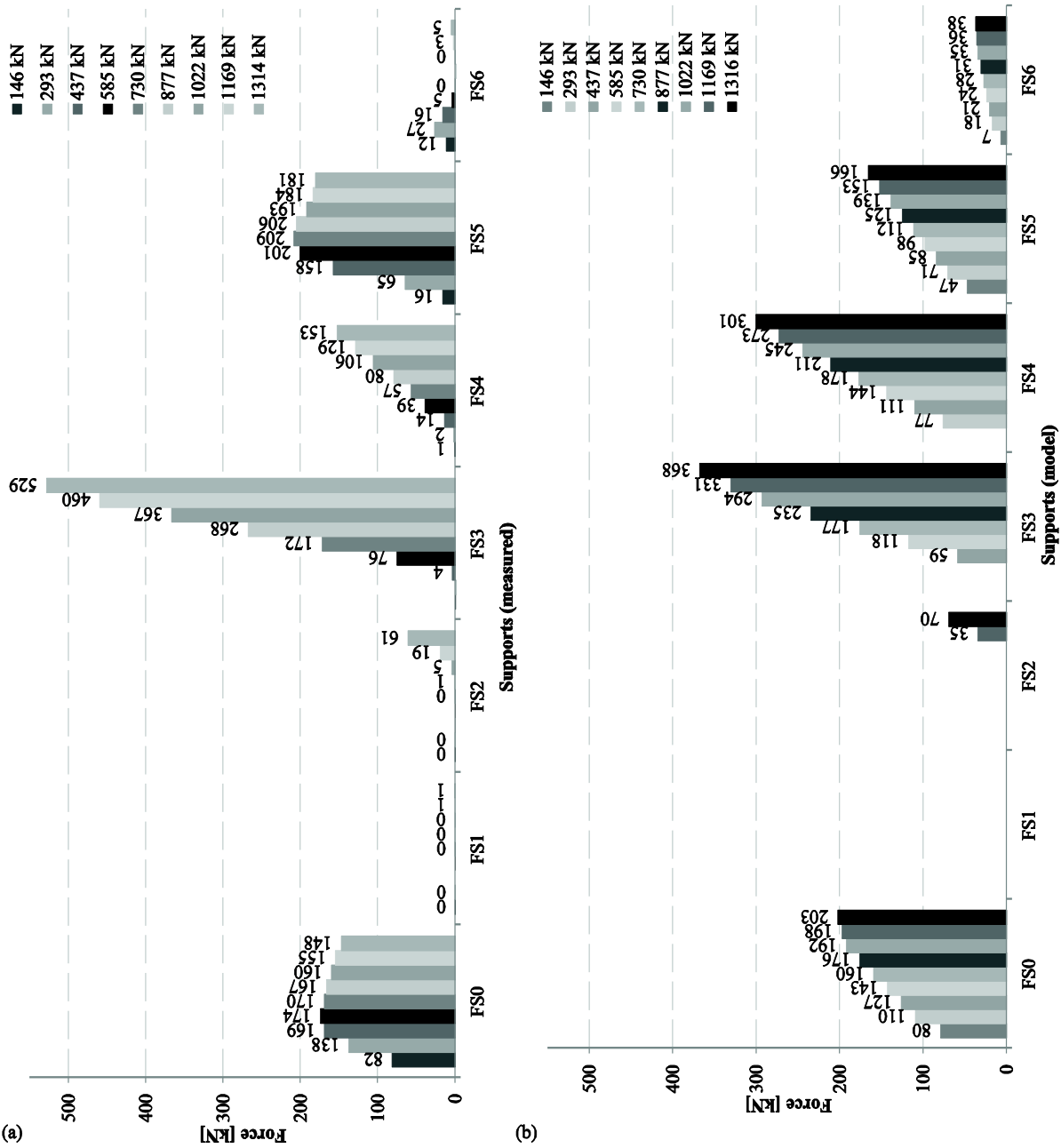
35 A similar approach is used to determine the applied total reaction force $F_{tot,4d}$ over $4d_l$:

36
$$F_{tot,4d} = FS3 + \frac{351 \text{ mm}}{358 \text{ mm}}(FS2 + FS4) = 739 \text{ kN} = 166 \text{ kip} \qquad (3)$$

37 Similarly, the average shear stress τ_{4d} over $4d_l$ can be defined as:

1

$$\tau_{4d} = \frac{F_{tot,4d}}{4d_l^2} = \frac{739 \text{ kN}}{4(265 \text{ mm})^2} = 2.63 \text{ MPa} = 381 \text{ psi} \qquad (4)$$

2

3
4 **FIGURE 5 Reaction forces at 9 intervals of 10% of the ultimate concentrated load: (a) as
5 measured by the load cells; (b) as found in linear finite element calculation assuming
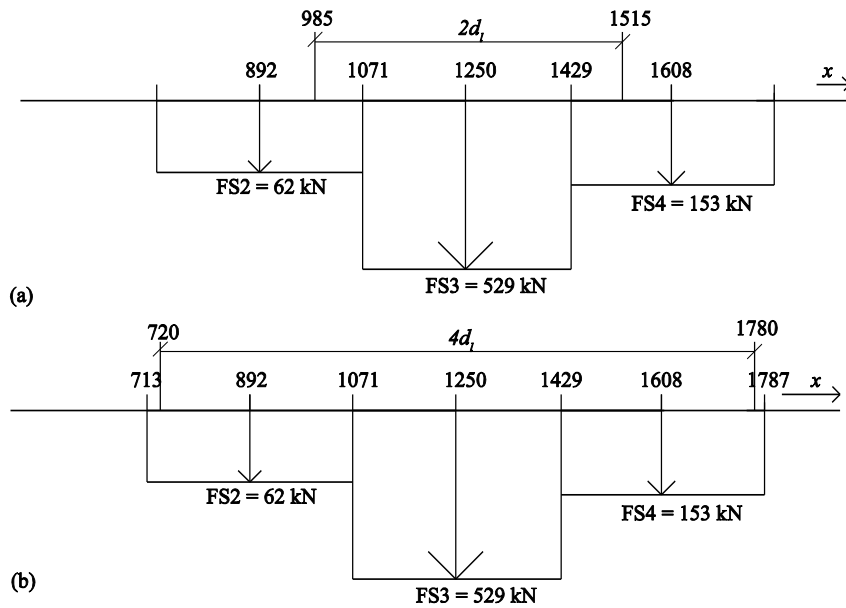6 phased activation of the supports.**
7 **NOTE: 1 kN = 0.225 kip.**

8

1
2
3 **FIGURE 6 Method for determining the shear stress around the peak of the measurement;**
4 **x-axis along width, distances in [mm], forces in [kN]: (a) assuming a distribution width of**
5 **$2d_l$; (b): assuming a distribution width of $4d_l$.**
6 **NOTE: 1 mm = 0.04 in. and 1 kN = 0.225 kip.**
7
8 When the results from the finite element model are analyzed, the average shear stress over the
9 assumed distribution width can be determined from two methods:
10   1. By integrating the shear stresses (eg. Fig. 7) over the considered distribution width to
11   determine the shear force at the support, which is then divided by the distribution width
12   and the effective depth, and
13   2. Based on the reaction forces in the discrete supports; this approach is similar to the
14   interpretation of the experimental results (Fig. 6a and Fig. 6b).
15 At a concentrated load of F_{jack} = 585 kN (132 kip), the stress distribution (with the peak at the
16 location of the concentrated load) at the support in the finite element model is shown in Fig. 7.
17 Integrating the shear stress over $2d_l$ results in τ_{2d} = 1.30 MPa (189 psi) and integrating over $4d_l$
18 results in τ_{4d} = 1.10 MPa (160 psi).
19
20 **TABLE 3 Overview of results for the comparison of the experimental shear stresses over**
21 **$2d_l$ and $4d_l$ to the finite element model. Results for two load levels: 40% and 90% of the**
22 **ultimate load.**

Concentrated load	585 kN (132 kip)		1314 kN (296 kip)	
Shear stress	τ_{2d} MPa (psi)	τ_{4d} MPa (psi)	τ_{2d} MPa (psi)	τ_{4d} MPa (psi)
Measurements	1.51 (219)	0.87 (126)	4.13 (599)	2.63 (381)
Model, integrating stresses	1.30 (189)	1.10 (160)	3.28 (476)	2.70 (392)
Model, reaction forces	1.39 (202)	1.27 (184)	3.25 (471)	2.60 (377)

23
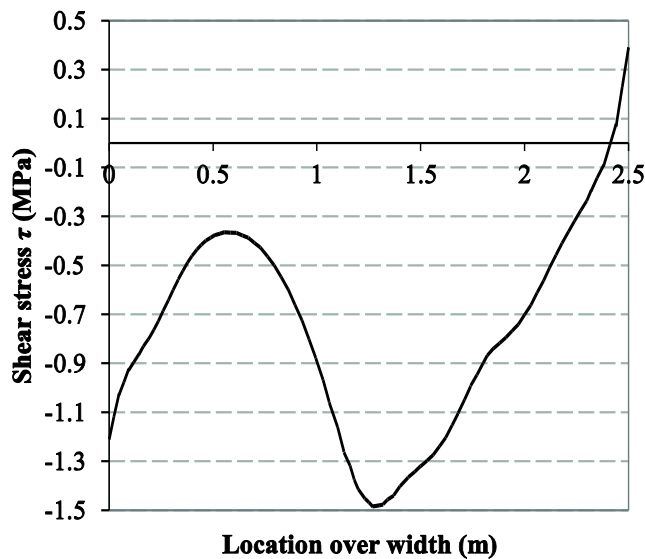
1
2 **FIGURE 7 Shear stress distribution at the support in the finite element model.**
3 **NOTE: 1 m = 3.3 ft, 1 MPa = 145 psi.**
4
5 An overview comparing the results in the experiment to those from the finite element model is
6 given in Table 3 for 40% of the ultimate experimental load (F_{jack} = 585 kN = 132 kips) and 90%
7 of the ultimate load (F_{jack} = 1314 kN = 296 kips). In Table 3, the resulting shear stress is given
8 based on the measured reaction forces in the experiments, based on the method of integrating the
9 shear stress distribution from the finite element model and based on the reaction forces given in
10 the finite element model. The results in Table 3 show that distributing the peak shear stress over
11 $4d_l$ gives a conservative estimate of the shear stress in the finite element model as compared to
12 the shear stress based on the reaction forces in the experiment. The results on the last two rows in
13 Table 3 also show similar shear stresses when the approach is based on the reaction forces from
14 the finite element model or from the resulting shear stress distribution in the model.
15
16 **CASE STUDY**
17 To complete this study, a comparison between the Quick Scan result and the Unity Check based
18 on a linear finite element approach is carried out for the case of an existing continuous solid slab
19 bridge built in 1959. The case under study has 4 spans, with end spans of 10.1 m (33.1 ft) and
20 mid spans of 14.4 m (47.2 ft) and a width of 10 m (32.8 ft) of which 6 m (19.7 ft) carries traffic.
21 The depth of the slab varies transversely from 530 mm (20.9 in.) to 470 mm (18.5 in.) and at the
22 edges from 670 mm (26.4 in.) to 735 mm (28.9 in.). The depth varies longitudinally from 550
23 mm (21.7 in.) at the supports to 530 mm (20.9 in.) at mid span. Plain rebars of QR24 with a
24 yield strength of 240 MPa (34.8 ksi) were used. The cover to the reinforcement is 25 mm (0.98
25 in.). The sagging moment reinforcement ratio in the end span is ρ = 0.69% and the hogging
26 moment reinforcement ratio at the mid supports is ρ = 0.78%. As for the existing slab bridges
27 from The Netherlands owned by the Dutch Ministry of Infrastructure and the Environment, the
28 characteristic cylinder compressive strength of the concrete can be assumed as f_{ck} = 35 MPa
29 (5076 psi) (*14*).
30 The Quick Scan approach results in unity checks for three cross-sections. The finite
31 element results, on the other hand, can be used to verify every cross-section in the studied spans.

1   For the considered case, the governing cross-section in the Quick Scan is at support 2-3 (near the
2   mid support in the mid span) with a shear stress due to composite dead load and live loads from
3   Load Model 1 at the edge of the support v_{Ed} = 0.68 MPa (99 psi) and a shear capacity $v_{Rd,c}$ = 0.91
4   MPa (132 psi) (the lower bound shear capacity v_{min} as determined in (15) is governing over $v_{Rd,c}$
5   from EN 1992-1-1:2005 (2)). These stresses result in a Unity Check value of UC = 0.74.
6   Consequently, a linear finite element model of the considered bridge is used as a next
7   level of approximation. The slab is modeled as a plate with shell elements. The variable depth in
8   the transverse direction is taken into account, while the variable depth in the longitudinal
9   direction is not considered. The governing shear force in the finite element model is found to be
10   278 kN/m (19 kip/ft). The shear capacity is again determined by the lower bound of the shear
11   stress v_{min} (15) and results in V_{min} = 438 kN/m (30 kip/ft). The resulting Unity Check at the
12   governing section is then UC = 0.63.
13   This comparison shows that the goal of the finite element model as a next level of
14   approximation –to be a more selective assessment tool than the Quick Scan method- is met. The
15   Quick Scan is based on a series of conservative assumptions that cover the entirety of all solid
16   slab bridges owned by the Dutch Minsitry of Infrastructure and the Environment. For individual
17   cases, the assumptions can often prove to be overly conservative. This observation is reflected by
18   the smaller Unity Check found from the finite element model, and is according to the philosophy
19   of the levels of approximation as described by the *fib* Model Code 2010 (3).
20
21   **SUMMARY AND CONCLUSIONS**
22   For the assessment of existing reinforced concrete solid slab bridges in the Netherlands, the first
23   level of approximation is a spreadsheet-based calculation, the Quick Scan. Within the scope of
24   the Quick Scan, an effective width needs to be determined over which the wheel loads can be
25   distributed to calculate their contribution to the resulting shear stress. It is found, based on the
26   results of a series of experiments on slab strips with increasing widths, based on a statistical
27   analysis and based on nonlinear finite element calculations, that the effective width for use in the
28   Quick Scan and other hand calculation methods can be determined based on an assumption of
29   horizontal load spreading from the far side of the loading plate to the face of the support under an
30   angle of 45 degrees.
31   If a bridge fails to meet the criteria of the Quick Scan, a more refined analysis needs to be
32   carried out by means of a finite element analysis. When interpreting the results from the finite
33   element analysis for assessment, the key question is how to distribute the peak shear stress over
34   the support to obtain the design shear stress. Based on a comparison between the measurements
35   of reaction forces in an experiment and a corresponding finite element model, it is shown that in
36   finite element models the peak shear stress at the support can be distributed over a width of $4d_l$
37   and that conservative results are still obtained.
38   These recommendations for the distribution of the shear stress at the support are applied
39   to a case of an existing solid slab bridges. It is found that the considered Levels of
40   Approximation perform well when these recommendations are taken into account.
41
42
43   **ACKNOWLEDGEMENT**
44   The authors wish to express their gratitude and sincere appreciation to the Dutch Ministry of
45   Infrastructure and the Environment (Rijkswaterstaat) for financing this research work and

InfraQuest for coordinating the cooperation between Delft University of Technology, Rijkswaterstaat and the research institute TNO.

REFERENCES

1. CEN, Eurocode 1: Actions on structures - Part 2: Traffic loads on bridges, *EN 1991:2-2003*. 2003, Comité Européen de Normalisation: Brussels, Belgium. p. 168.
2. CEN, Eurocode 2: Design of Concrete Structures - Part 1-1 General Rules and Rules for Buildings. EN 1992-1-1:2005. 2005, Comité Européen de Normalisation: Brussels, Belgium. p. 229.
3. fib, *Model code 2010: final draft*. Lausanne: International Federation for Structural Concrete, 2012.
4. Goldbeck, A.T., The influence of total width on the effective width of reinforced concrete slabs subjected to central concentrated loading. *ACI Journal Proceedings*, Vol. 13, No. 2, 1917, pp. 78-88.
5. Coin, A. and Thonier, H., Experiments on the shear capacity of reinforced concrete slabs. *Annales du batiment et des travaux publics*, 2007, pp. 7-16. (in French)
6. Lantsoght, E.O.L., van der Veen, C., and Walraven, J.C., Shear in One-way Slabs under a Concentrated Load close to the support. *ACI Structural Journal*, Vol. 110, No. 2, 2013, pp. 275-284.
7. Lantsoght, E.O.L., Shear tests of reinforced concrete slabs and slab strips under concentrated loads. *Proceedings of The 9th fib International PhD Symposium in Civil Engineering*, Karlsruhe Institute of Technology (KIT), Karlsruhe, Germany, 2012, pp. 3-8.
8. Lantsoght, E.O.L., van der Veen, C., and Walraven, J.C., Shear assessment of solid slab bridges. *ICCRRR 2012, 3rd International Conference on Concrete Repair, Rehabilitation and Retrofitting*, Cape Town, South Africa, 2012, pp. 827-833.
9. Lantsoght, E.O.L., Van der Veen, C., and Walraven, J.C., Shear Capacity of Slabs under a Combination of Loads. *fib Symposium: Engineering a concrete future: technology, modeling and construction*, Tel Aviv, 2013, pp. 297-300.
10. TNO DIANA, Users Manual of DIANA, Release 9.4.4. 2012: Delft, The Netherlands, http://www.tnodiana.com
11. Regan, P.E., *Shear resistance of members without shear reinforcement; proposal for CEB Model Code MC90*. 1987, Polytechnic of Central London: London, UK. p. 28.
12. Lantsoght, E.O.L., Shear in Reinforced Concrete Slabs under Concentrated Loads Close to Supports.Delft University of Technology; PhD Thesis, 2013. p. 340.
13. Doorgeest, J., *Transition between one-way shear and punching shear*. Delft University of Technology. MSc Thesis, 2012, p. 215.
14. Steenbergen, R.D.J.M. and Vervuurt, A.H.J.M., Determining the in situ concrete strength of existing structures for assessing their structural safety. *Structural Concrete*, Vol. 13, No. 1, 2012, pp. 27-31.
15. Walraven, J.C., *Minimum shear capacity of reinforced concrete slabs without shear reinforcement: the value v_{min}*. 2013. p. 20 (in Dutch).